ADAM33 Enzyme Properties and Substrate Specificity

Jun Zou,* Rumin Zhang, Feng Zhu, Jianjun Liu, Vincent Madison, and Shelby P. Umland

Schering-Plough Research Institute, 2015 Galloping Hill Road, Kenilworth, New Jersey 07033

Received November 9, 2004; Revised Manuscript Received January 6, 2005

ABSTRACT: ADAM33 is an asthma susceptibility gene recently identified through a genetic study of asthmatic families [van Eerdewegh, et al. (2002) *Nature 418*, 426−430]. To understand the function of the gene product, the recombinant metalloproteinase domain of human ADAM33 was purified and tested for its substrate cleavage specificity using peptides derived from β-amyloid precursor protein (APP). A single Ala substitution at the P2 position of a 10-residue APP peptide, YEVHH*QKLVF, yielded a 20-fold more efficient substrate. Terminal truncation studies identified a minimal nine-residue core (P5−P4′) important for ADAM33 recognition and cleavage. Full positional scanning of the 10-mer peptide using the 19 naturally occurring L-amino acids (excluding Cys) revealed a substrate specificity profile. A strong preference for Val or Ile at P3, Ala at P2, and Gln at P1′ was observed. The substrate binding model based on the X-ray structure of the ADAM33−inhibitor complex supported the observed substrate specificity profile. On the basis of this, an improved substrate was designed and a fluorescence resonance energy transfer (FRET) assay was developed using a fluorogenic derivative of this substrate. Kinetic studies confirmed that the best substrate, FRET-P2 [K(Dabcyl)YRVAF*QKLAE(Edans)K], was ∼100-fold more efficient than the wild-type APP peptide substrate, with a k_{cat}/K_m value of $(3.6 \pm 0.1) \times 10^4$ s^{-1} M^{-1}. Using this substrate and the FRET assay, ADAM33 enzyme activity and thermal stability were characterized. ADAM33 dependence on buffer conditions, detergents, and temperature was examined, and optimal conditions were defined. Accurate K_i values for tissue inhibitors of metalloproteinase and small molecule compounds were obtained.

ADAM33[1] (a disintegrin and metalloprotease) is an asthma susceptibility gene identified by a genetic linkage and polymorphism study of asthmatic families (*1*). ADAM33 belongs to a family of type I transmembrane metalloproteinases which share a conserved structure with multiple domains: an N-terminal secretion signal sequence, pro and catalytic domains, disintegrin, and cysteine-rich domains which are usually followed by an EGF repeat, a transmembrane, and a carboxyl-terminal cytoplasmic tail (*2*). Approximately half the ADAM family members, including ADAM33, contain an active site HEXXHXXGXXH consensus sequence of a zinc binding motif and a glutamic acid in the catalytic domain, which was predicted as a key feature for being an active metalloproteinase (*3*, *4*). A major function of those active ADAMs is proteolytic release of cell surface membrane proteins such as cytokines, growth factors, and receptors (*2*, *5*). ADAM17/TNF-α converting enzyme (TACE), one of the best studied ADAMs, sheds soluble TNF-α after cleavage of the membrane-anchored precursor (*6*). ADAM17 also processes several other integral membrane proteins such as amyloid precursor protein (APP) (*7*), transforming growth factor-α (TGF-α), and L-selectin (*8*).

ADAM33 belongs to a subfamily as determined by sequence homology, which includes ADAM19, ADAM12, and ADAM13 (*1*, *9*, *10*). Recombinant ADAM19 metalloproteinase was able to cleave peptides corresponding to the known cleavage sites of TNF-α, TRANCE, and KL-1 (*11*). Overexpression of ADAM19 in L929 cells suggested that ADAM19 may participate in the shedding of β1-neuregulin, a member of the epidermal growth factor family (*12*). ADAM12 was reported to process heparin-binding epidermal growth factor (HB-EGF) in vivo (*13*) and to cleave insulin-like growth factor binding proteins 3 and 5 (*14*). We have previously demonstrated that ADAM33 is an active proteinase which was able to cleave α2-macroglobulin (*15*) and synthetic peptides (*16*). The enzymatic activity of ADAM33 can be inhibited by a tissue inhibitor of metalloproteinases 3 and 4 (TIMP-3 and -4, respectively) as well as several small molecules (*16*). However, it is still unknown what the physiological substrates and functions of ADAM33 are, and what the role of ADAM33 is in the pathophysiology of asthma. ADAM33 was primarily expressed in lung fibroblasts and bronchial smooth muscle cells (*1*, *17*) and was hypothesized to be involved in bronchial tissue remodeling in asthmatics (*18*). The X-ray crystal structure of the ADAM33 catalytic domain that we reported recently revealed the Zn-coordinated active site and polypeptide fold, which resembled that of other metalloproteinases, while the substrate-binding site contained unique features that allow for structure-based design of specific inhibitors of this enzyme (*19*).

* To whom correspondence should be addressed. Telephone: (908) 740-6578. Fax: (908) 740-3918. E-mail: jun.zou@spcorp.com.

[1] Abbreviations: ADAM, a disintegrin and metalloproteinase; BSA, bovine serum albumin; MMP, matrix metalloproteinase; KL-1, kit-ligand-1; APP, amyloid precursor protein; TRANCE, TNF-related activation-induced cytokine; TNF-α, tumor necrosis factor-α; TACE, tumor necrosis factor-α converting enzyme; TGF-α, transforming growth factor-α; HB-EGF, heparin-binding epidermal growth factor; TIMP, tissue inhibitor of metalloproteinase; Ni−NTA, nickel−nitrilotriacetic acid; FRET, fluorescence resonance energy transfer; HPLC, high-performance liquid chromatography; RT, room temperature; FMOC, 9-fluorenylmethoxycarbonyl; TFA, trifluoroacetic acid; wt, wild type.

10.1021/bi0476230 CCC: $30.25
Published on Web 02/19/2005

In our previous study, we expressed and purified a soluble recombinant form of human ADAM33 catalytic protein and used it to search for cleavable substrates by testing a number of synthetic peptides, most of which were derived from the known cleavage sites of shed membrane proteins (*16*). Four peptide substrates, KL-1, APP, insulin B-chain, and TRANCE, were identified which were cleaved by ADAM33. Kinetic studies indicated that cleavages of these substrates by ADAM33 were not very efficient. In this report, we have established a substrate specificity profile of ADAM33 protease activity by an alanine scan of the wild-type APP peptide and full positional scan of the substituted APP peptide. We have generated a highly efficient substrate through a combination of amino acid substitutions of the APP peptide. With this substrate, properties of ADAM33 were characterized and the effects of pH, ionic strength, detergents, and temperature on catalytic activity were examined. Sensitivity of ADAM33 activity to TIMPs and small molecule inhibitors was also tested.

MATERIALS AND METHODS

Reagents. All chemicals were from Sigma-Aldrich (St. Louis, MO) unless indicated otherwise. Human tissue inhibitors of metalloproteinase (TIMPs) were purchased from R&D Systems (Minneapolis, MN). All reagents and media for *Drosophila* S2 cell expression were from Invitrogen (Carlsbad, CA). Small molecule inhibitors IK682 (*20*) and marimastat (*21*) were synthesized by Medicinal Chemistry at Schering Plough Research Institute.

Expression and Purification of the Recombinant Human ADAM33 Catalytic Domain. The details of expression and purification of the recombinant human ADAM33 catalytic domain have been described previously (*16*). In brief, ADAM33 pro and catalytic domains (nucleotides 91−1227, corresponding to amino acids L31−P409) were cloned into an inducible expression vector, pMT/Bip/V5-His-C (Invitrogen), and attached with a V5-6xHis tag on its 3′ end. The stable transfected *Drosophila* S2 cell line was generated and maintained at 23 °C in DES medium containing 10% fetal bovine serum (FBS), 0.1% Fluronic F-68, and 300 μg/mL hygromycin B. Expression of the human ADAM33 protein was induced in the presence of 10 μM $CdCl_2$ and 200 μM $ZnCl_2$ in serum-free medium. The ADAM33 catalytic domain in conditioned medium after induction for 6 days was first enriched with a SP-Sepharose Fast Flow column, followed by a Ni−NTA column, and finally purified to homogeneity by a Superdex-75 column, using the AKTA FPLC system (Amersham-Pharmacia Biotech, Piscataway, NJ). The N-terminal amino acid sequence of the ADAM33 protein was confirmed by protein sequencing (*22*). The protein concentration of the ADAM33 catalytic domain was estimated by UV absorption using a molar extinction coefficient ϵ_{280} of 26 780 M^{-1} cm^{-1} (*16*). The active enzyme concentration of ADAM33 was determined by the inhibitor titration of the active site as described in ref *16*. The enzyme was diluted in the enzyme dilution buffer [40 mM HEPES (pH 7.0), 20 μM $CaCl_2$, 20 μM $ZnCl_2$, 0.001% Brij35, 0.2 mg/mL BSA, and 10% glycerol] before being used.

Peptide Synthesis. Peptides were synthesized in-house. Fmoc chemistry was used on either an ABI model 431A peptide synthesizer (Applied Biosystems, Foster City, CA) or an ACT model 496 multiple synthesizer (Advanced ChemTech, Louisville, KY). The molecular masses of purified peptides were confirmed by electrospray ionization mass spectrometry.

Peptide Cleavage Assay. The peptide substrate (50 μM) was incubated with or without ADAM33 (4−80 nM) in assay buffer [20 mM HEPES (pH 7.0), 0.5 M NaCl, and 0.2 mg/mL BSA] for 1−2 h at room temperature (RT). The reaction was quenched by adding 10% trifluoroacetic acid (TFA) to a final concentration of 1%, and samples were analyzed on an Agilent model 1100 HPLC system with a C8 column [4.6 mm (inside diameter) × 50 mm (length)]. Solvents were as follows: (A) 0.1% TFA in water and (B) 0.09% TFA in acetonitrile. A linear gradient from 2 to 42% B was carried out over 7 min at 1.5 mL/min, and the eluate was monitored at 214 nm. The percentage of peptide cleavage was calculated using the peak area of the cleaved products divided by the sum of the peak areas of both the products and the remaining substrate. The cleavage sites of the peptide were identified by either electrospray (ES) or matrix-assisted laser desorption ionization time-of-flight (MALDI-TOF) mass spectrometry.

Kinetic Studies. Kinetic constants of peptide substrates were obtained by using the HPLC assay described above and analysis as reported previously (*23*−*25*). In brief, ADAM33 (4 nM) was incubated with peptide substrate (5−250 μM) in assay buffer for 10−60 min at RT. Reactions were timed to allow less than 15% turnover of the substrate. The initial cleavage velocities of the peptides were obtained by plotting cleaved product versus reaction time. The kinetic constants (k_{cat}, K_m, and k_{cat}/K_m) were determined using Prism version 3.0 (GraphPad, San Diego, CA) based on a best fit of the data with the Michaelis−Menten equation (*26*).

Fluorescence Resonance Energy Transfer (FRET) Assay. Fluorogenic substrates, FRET-P1 [K(Dabcyl)-YEVAH*QKLAE(Edans)K] and FRET-P2 [K(Dabcyl)-YRVAF*QKLAE(Edans)K], based on the modified peptide APP sequence were synthesized and used to measure ADAM33 enzyme activity. The assay was carried out in 4 nM enzyme and 30 μM substrate in an assay buffer consisting of 20 mM HEPES (pH 7.0), 0.5 M NaCl, and 0.2 mg/mL BSA. The initial reaction velocity was measured at excitation and emission wavelengths of 340 and 505 nm, respectively, with a GEMINI fluorescence reader (Molecular Devices, Sunnyvale, CA) for 15 min.

The inhibition dissociation constants (K_i) for inhibitors were determined according to the methods described previously (*24*, *27*). In brief, the FRET assay was performed in the presence or absence of inhibitors at RT using ADAM33 (4 nM) and FRET-P2 substrate (30 μM). For testing the tissue inhibitor of metalloproteinases (TIMPs), ADAM33 and human TIMPs were preincubated for 1 h at RT. Serial dilutions of TIMPs or synthetic inhibitors were tested starting at 8 μM (TIMP-2), 4 μM (TIMP-3 and -4), 2 μM (TIMP-1 and IK682), or 20 μM (marimastat). The initial velocities were plotted as a function of inhibitor concentration. For tight binding inhibitors (IK682 and TIMP-3 and -4), the apparent inhibitor dissociation constants (K_i^{app} values) were calculated by fitting the curve to the following modified Morrison's equation (*28*) with Prism version 3.0:

$$v_i = v_o\{[(E_o - I_o - K_i^{app})^2 + 4K_i^{app}E_o]^{1/2} + (E_o - I_o - K_i^{app})\}/2E_o$$

where $K_i^{app} = K_i(1 + S/K_m)$, v_o is the uninhibited initial velocity, v_i is the initial velocity in the presence of inhibitor at any given inhibitor concentration I_o, and E_o is the initial enzyme concentration. For all other less potent inhibitors, the inhibitor dissociation constants (K_i values) were determined by fitting the data to the rearranged Michaelis−Menten equation (*26*) for competitive inhibitor kinetics:

$$v_i = V_{max}S/[K_m(1 + I/K_i) + S]$$

Dependence of ADAM33 Activity on pH and Ionic Strength (NaCl, $ZnCl_2$, and $CaCl_2$) and Others. The pH dependence experiments were performed in 20 mM buffer (MES for pH 4.0, 5.0, 6.0, and 6.5, HEPES for pH 7.0, 7.5, and 8.0, and CHES for pH 8.5, 9.0, and 10.0) with 0.5 M NaCl. The NaCl dependence experiments were performed in 20 mM HEPES (pH 7.5). The experiments for other factors ($ZnCl_2$, $CaCl_2$, Brij35, glycerol, DMSO, and BSA) were carried out in the core buffer [20 mM HEPES (pH 7.5) and 0.5 M NaCl].

Temperature Dependence Experiments. Initial rates of product formation were determined at each temperature in the assay buffer [20 mM HEPES (pH 7.0) and 0.5 M NaCl] with a GEMINI fluorescence reader. To determine the enzyme stability at different temperatures, ADAM33 (80 nM) was preincubated in the assay buffer for a period of time: 0−150 min at 25 °C, 0−60 min at 30 °C, 0−40 min at 37 °C, 0−15 min at 45 °C, and 0−15 min at 55 °C. Aliquots of ADAM33 were removed at different time points and frozen at −80 °C, and were later diluted 10-fold to measure their protease activity. The curve summarizing the decay of protease activity with time was used to estimate the half-life of the activity at different temperatures by GraphPad Prism version 3.0.

RESULTS

We have previously reported that from testing more than 40 potential candidate peptides, four peptides were identified that were cleaved by ADAM33 (*16*). The rank order of relative cleavage efficiencies of these four peptides by ADAM33 was as follows: KL-1 > APP > insulin B-chain = TRANCE. The efficiency of cleavage of each (k_{cat}/K_m up to 3×10^2 s^{-1} M^{-1}) was lower than that of authentic biological substrates of other ADAM proteases (*23*, *29*). To study the impact of peptide sequence variation on the cleavage efficiency and substrate specificity, we explored the structure−activity relationship (SAR) of two ADAM33 peptide substrates by alanine-scan mutagenesis, initially with KL-1 (*16*) and with APP in this study.

Alanine Scan of the APP Peptide Substrate. The individual amino acids of the 10-mer peptide of APP, YEVHH*QKLVF, were substituted with alanine to assess the relative contributions of the amino acid side chains (Figure 1). Remarkably, cleavage of the P2-altered peptide substrate, in which Ala was substituted for His, was enhanced ~20-fold, whereas Ala substitution at P4′ increased cleavage efficiency less than 2-fold. In contrast, replacement of each amino acid at P5, P1′, and P2′ resulted in a more than 10-fold decrease in cleavage activity. Ala substitutions at the remaining positions had a relatively weaker effect on cleavage efficiency.

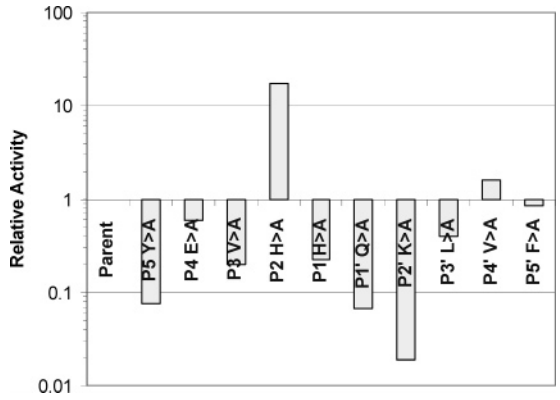

FIGURE 1: Alanine scan of the APP peptide substrate. On the basis of the 10-mer peptide sequence of APP, YEVHH*QKLVF, a series of peptides in which each of the 10 amino acids in the peptide was substituted individually with Ala were derived and synthesized. The peptide substrates (50 μM) were incubated with ADAM33 (4 nM) in assay buffer [20 mM HEPES (pH 7.0), 0.5 M NaCl, and 0.2 mg/mL BSA] for 1−2 h at RT. The reaction was stopped and subjected to HPLC analysis (see Materials and Methods).

Table 1: Effect of APP Peptide Length on ADAM33 Cleavage Efficiency

	peptide substrate sequence[a]	relative cleavage efficiency[b]
P7−P7′	GSYEV**A**H*QKL**A**FFA	1.2
P5−P5′-a	YEV**A**H*QKL**A**F	1.1
P5−P5′	Ac-YEV**A**H*QKLVF-NH_2	1.0
P5−P4′	YEV**A**H*QKL**A**	0.9
P4−P4′	EV**A**H*QKL**A**	0.1
P3−P3′	Ac-V**A**H*QKL-NH_2	0.0

[a] The bold residues are the Ala substitutions from the wild-type APP sequence, YEVHH*QKLVF. The asterisks denote the cleavage sites. [b] The assay was performed with 10 nM ADAM33 and 50 μM peptide substrate at RT for 1 h, followed by HPLC analysis (see Materials and Methods).

Peptide Size. The relative cleavage efficiency was determined for a series of different length peptides in which amino acids were either truncated or extended from the amino or carboxy terminus of the P2/P4′-Ala-substituted APP peptide (Table 1). Increased length of the peptide as seen in the P7−P7′ peptide only slightly enhanced the cleavage efficiency (compared with that of P5−P5′-a). Terminal truncations to P4−P4′ and P3−P3′ peptides virtually eliminated the cleavability. Thus, the P5−P4′ peptide is the minimal size for ADAM33 recognition and cleavage.

Full Positional Scan of the APP Peptide To Probe the Structure−Activity Relationship (SAR). With the P5−P5′ template incorporating two favorable Ala substitutions at P2 and P4′, YEVAH*QKLAF, we performed a full positional scan by substituting at each position the 19 naturally occurring L-amino acids except the oxidation-prone Cys. The relative activity data are detailed in Figure 2A−J. Several points can be made from these data. P5 Tyr could be substituted with a large, aromatic residue (Trp or Phe). Smaller, aliphatic hydrophobic residues (Ile, Leu, Met, and Val) were also tolerated at the P5 position, maintaining 80−90% of the activity of the parent template. P4 Glu tolerated many substitutions except Trp. Basic residues (Arg and Lys), aliphatic residues (Ile, Leu, Met, and Val), and the polar Gln

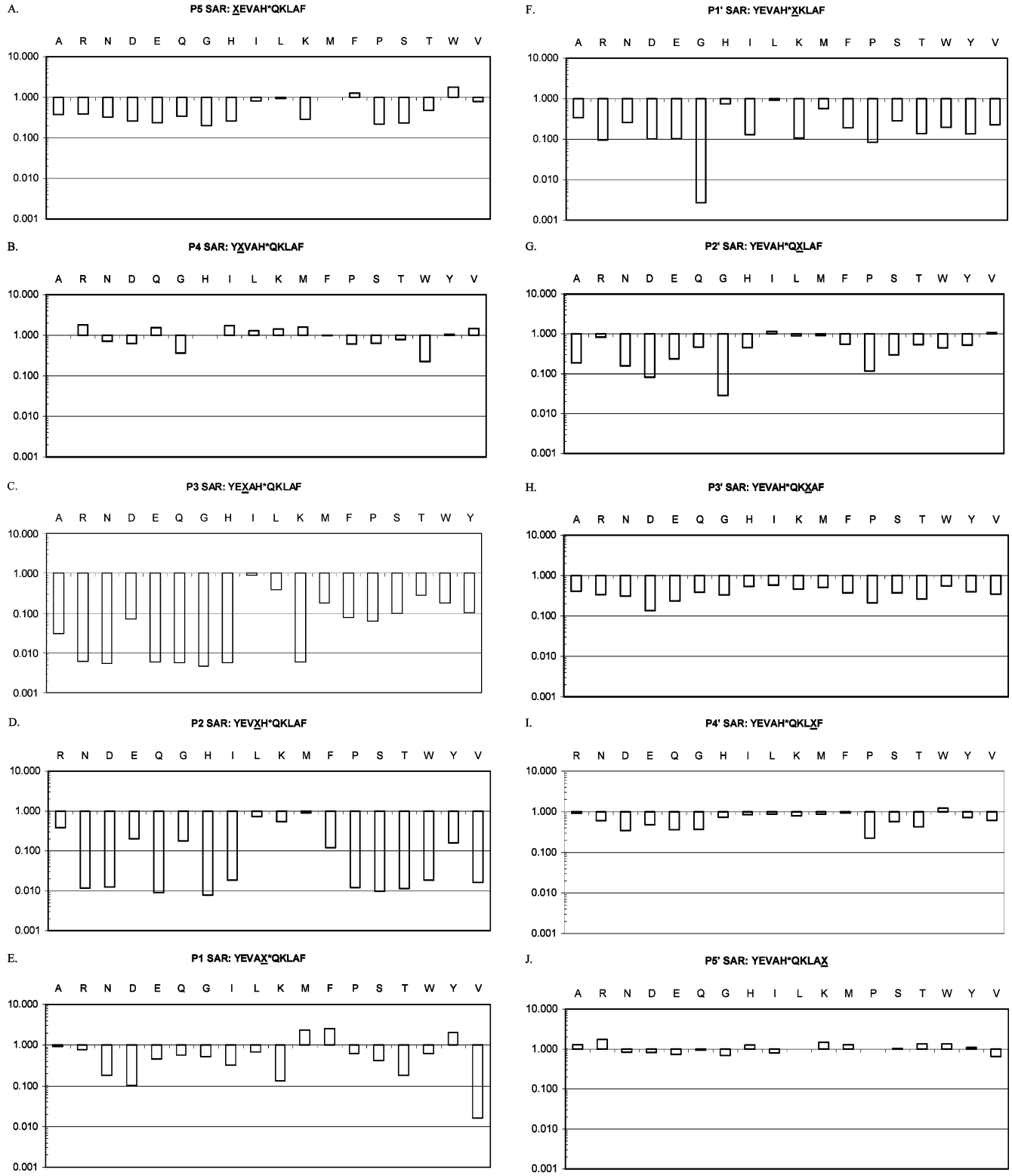

FIGURE 2: Full positional scan of the APP peptide as ADAM33 substrates to probe structure−activity relationship (SAR). Each position (*X*) of the P2/P4′-Ala-substituted APP peptide (YEVAH*QKLAF) was systematically replaced with the 19 naturally occurring L-amino acids (excluding Cys). The individually synthesized peptides (50 μM) were then subjected to the ADAM33 HPLC assay (see Materials and Methods). The relative activities compared to that of the template peptide are shown on the *Y*-axis.

residues were slightly more favored at the P4 position. The P3 position demonstrated a stringent requirement for Val. The small, β-branched Val could only be substituted with a slightly larger, β-branched sibling Ile. P2 Ala, identified earlier in an Ala-scan experiment (Figure 1), was the best residue at the P2 position. Substitution by Met, Leu, Lys, or Arg resulted in a loss of activity (10−60%). P1 His was inferior to Met, Phe, and Tyr. Ala, Arg, Gln, Glu, Gly, Leu, Pro, Ser, and Trp were also tolerated, with the activity within 2-fold of that of the parental peptide, although Val is prohibited at P1. At P1′ Gln, no equivalent or better substitutions were found, although Leu, Met, and His were suboptimal substitutions, which maintained 60−90% of the activity. P2′ Lys could be substituted with Arg or aliphatic

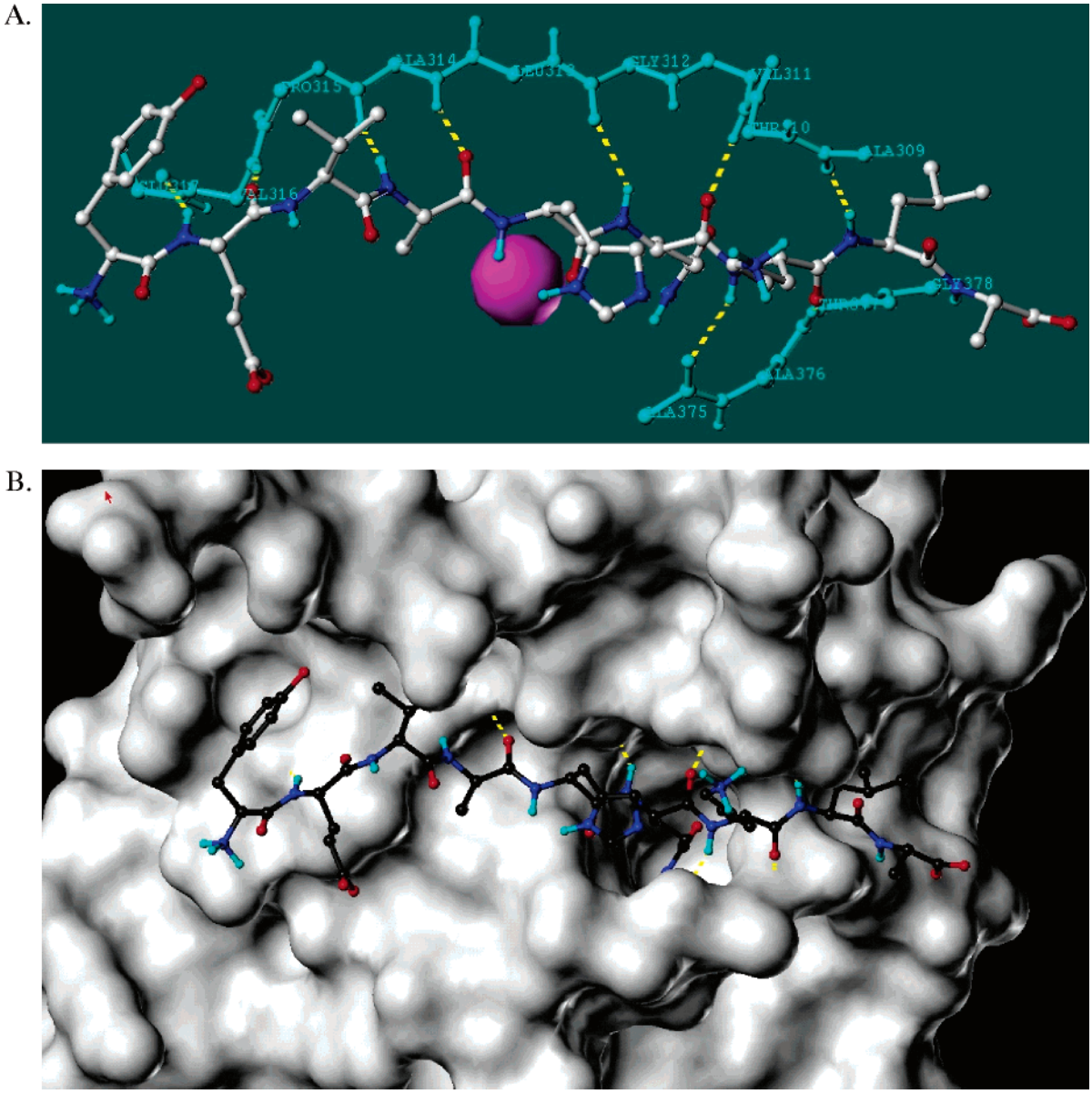

FIGURE 3: (A) Substrate YEVAHQKLA was docked into the ADAM33 protein from the X-ray structure of the ADAM33 complex with a prime-side hydroxamate inhibitor marimastat (*19*). The P2′ backbone was anchored at its position in the inhibitor, and the H-bonds of the P4, P2, P1′, P2′, and P3′ residues were also used as guidepoints. The figure shows the substrate in atom colors, the protein backbone of the two contacting β-strands in cyan, H-bonds in yellow, and the active site zinc in magenta. (B) YEVAHQKLA substrate docked into the ADAM33 protein. The figure shows the solvent-accessible surface of the protein (gray scale) and ball and stick representation of the substrate (atom colors with carbon black). The P5 residue faces a surface depression. P4 is solvent exposed beyond Cβ. P3 fits into a hydrophobic cavity covered by the Asn276-linked carbohydrate chain. P2 fits on top of the saddle point formed by the histidines ligating the catalytic zinc. P1 and P2′ extend out flanked by the protein wall toward the top of the figure. P1′ extends into a deep largely hydrophobic cavity; the Gln side chain could H-bond to Ala374 CO or the OH group of Thr310 or Thr377. P3′ packs against the right edge of the protein with one side solvent exposed. P4′ is solvent-exposed.

residues (Ile, Leu, Met, and Val). At P3′ Leu, was the best among all the residues, with many other residues being suboptimal replacements. P4′ Ala, identified in an Ala scan experiment (Figure 1), was the second best, after Trp; however, P4′ Ala could be replaced with many other residues. P5′ was the most permissive site for substitutions, which was consistent with an earlier C-terminal truncation study: the P5−P4′ peptide was almost as competent as the P5−P5′ peptide.

Modeling of ADAM33−Substrate Binding. An ADAM33−substrate binding model was established on the basis of the X-ray structure of the ADAM33−inhibitor complex (*19*), and the model was consistent with the experimental results observed upon alanine scan or full positional scan studies. As shown in Figure 3, large hydrophobic residues that could pack in the surface depression were preferred at P5, with Tyr preferred over Ala by ~10-fold (Figure 1). The P3 position favored small hydrophobic residues that could fit into the restricted S3 pocket with Val preferred over Ala by ~5-fold. The S2 saddle point severely restricted P2 in the vicinity of Cβ; unbranched residues were preferred except for γ-branched Leu, and Ala was preferred over His by ~20-fold. P1 and P2 fitted against a protein wall on one side, but the binding pocket was open at the top and on the other side. At P1, aromatic and hydrophobic residues were somewhat preferred; His was preferred over Ala by ~3-fold. P1′ fit in

Table 2: Steady-State Kinetic Parameters for Substituted APP Peptide Substrates Determined for ADAM33 Metalloproteinase

Substrate	Sequence[a]	*k*cat/*K*m[b] ($M^{-1}s^{-1}$)	Relative activity
APP-wt	$_{AC}$-YEVHH*QKLVF-$_{NH2}$	(1.6 ± 0.3) x 10^2	1
APP-AA	YEV**A**H*QKL**A**F-$_{OH}$	(7.2 ± 0.2) x 10^3	45
APP-AAE	**K**YEV**A**H*QKL**AEK**-$_{OH}$	(4.4 ± 0.2) x 10^3	28
APP-AFAE	**K**YEV**AF***QKL**AEK**-$_{OH}$	(1.0 ± 0.2) x 10^4	65
APP-RAFAE	**K**Y**R**V**AF***QKL**AEK**-$_{OH}$	(1.3 ± 0.2) x 10^4	79
FRET-P1	K(Dabcyl)YEV**A**H*QKL**AE**(Edans)K-$_{OH}$	(1.3 ± 0.4) x 10^4	83
FRET-P2	K(Dabcyl)Y**R**V**AF***QKL**AE**(Edans)K-$_{OH}$	(3.6 ± 0.1) x 10^4	230

[a] The bold residues are the Ala substitutions from the wild-type APP sequence. [b] Kinetic constants (mean ± SD) were determined by incubating ADAM33 (4 nM) with peptide (5−250 μM) in assay buffer for 10−60 min at RT, and product formation was assessed by HPLC. The Michaelis−Menten equation was used to calculate kinetic constants (see Materials and Methods).

an enclosed, largely hydrophobic site accommodating hydrophobic Leu and Met. Hydrogen bonding to Ala374 CO and the OH group of Thr310 or Thr377 could help stabilize the Gln and His side chains; Gln was preferred over Ala by ~10-fold. At P2′, larger aromatic/hydrophobic residues and the long aliphatic chains of Arg and Lys were preferred and Lys was preferred over Ala by ~20-fold. The P4, P3′, P4′, and P5′ side chains were largely exposed and exhibited little preference for any residue.

Kinetic Study of Substituted Peptide Substrates. Through various combinations of amino acid substitutions, peptide substrates with improved efficiency were identified. Kinetic constants of representative peptide substrates were determined and listed in Table 2. Double Ala substitutions at P2 and P4′ of the original APP peptide significantly enhanced the substrate cleavage with a k_{cat}/K_m value of (7.2 ± 0.2) × 10^3 s^{-1} M^{-1} (APP-AA, 45-fold increase relative to that of wild-type APP). To increase the solubility, Phe at P5′ was replaced with Glu and a Lys residue was added to each end of the peptide which slightly reduced the substrate cleavage efficiency (APP-AAE, 28-fold relative to that of wild-type APP). Additional replacements of His with Phe at P1 and Arg with Glu at P4 enhanced cleavage efficiency 79-fold for the peptide APP-RAFAE, with k_{cat}/K_m value of (1.3 ± 0.2) × 10^4 s^{-1} M^{-1}. Two peptides were labeled with a fluorophore and quencher, Edans and Dabcyl, respectively, to make fluorogenic substrates for a fluorescence resonance energy transfer (FRET) assay. Interestingly, a combination of amino acid substitutions and addition of Edans and Dabcyl increased cleavage efficiency. The best substrate, FRET-P2, demonstrated a cleavage efficiency 230-fold greater than that of wild-type APP, with a k_{cat}/K_m value of (3.6 ± 0.1) × 10^4 s^{-1} M^{-1}.

Dependence of ADAM33 Activity on pH, Ionic Strength (NaCl, $ZnCl_2$, and $CaCl_2$), and Others. Using two fluorescent peptide substrates (FRET-P1 and FRET-P2), a FRET assay was developed to measure ADAM33 protease activity. The pH and NaCl dependence of ADAM33 activity is shown in Figure 4. Interestingly, the two substrates had distinct

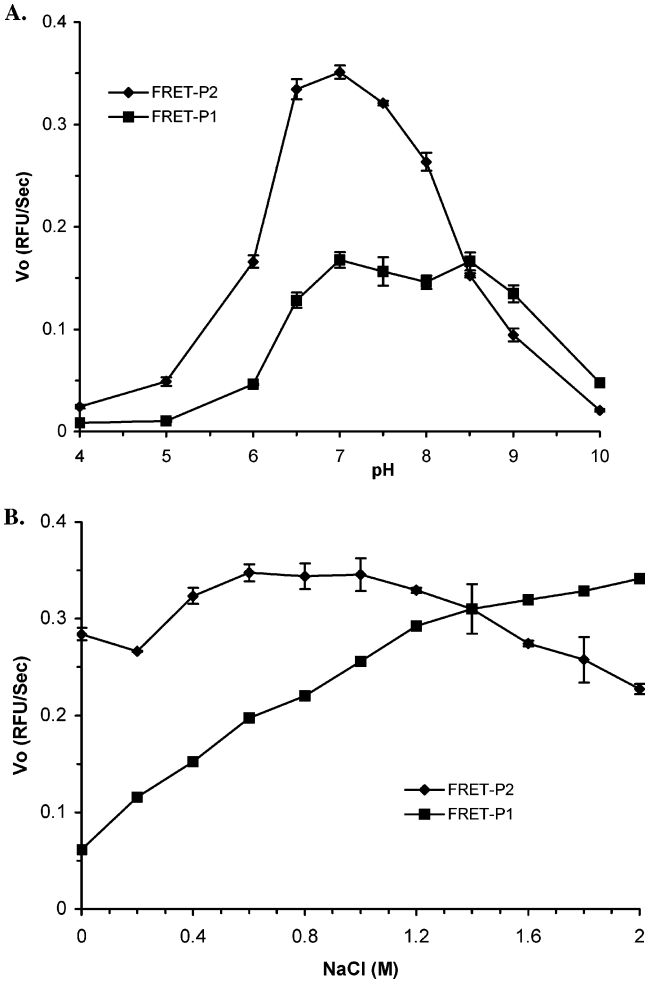

FIGURE 4: Dependence of ADAM33 protease activity on pH (A) and NaCl concentration (B). Two fluorogenic substrates, FRET-P1 [K(Dabcyl)YEVAH*QKLAE(Edans)K] and FRET-P2 [K(Dabcyl)YRVAF*QKLAE(Edans)K], were used to measure ADAM33 enzyme activity by the FRET assay. The experiments were performed using 10 nM enzyme and 30 μM substrates in 20 mM buffer, 0.5 M NaCl (for pH dependence), or 20 mM HEPES at pH 7.0 (for NaCl dependence) and RT (see Materials and Methods). The initial reaction velocity (V_o) was measured as relative fluorescence units per second (RFU/s) at excitation and emission wavelengths of 340 and 505 nm, respectively, with a GEMINI fluorescence reader.

profiles: FRET-P2 displayed higher activity with a pH optimum range of 6.5−7.5; in contrast, FRET-P1 had a broader but lower activity profile with an optimal pH range of 6.5−9.0. The sensitivity to NaCl was also different for two substrates: the extent of cleavage of FRET-P1 was directly proportional to NaCl concentration up to 2 M, while FRET-P2 was less sensitive to increases in the NaCl concentration. Due to the profile with a 2-fold higher activity at neutral pH and a 2−3-fold higher activity at low NaCl concentrations, FRET-P2 was chosen as a preferred substrate for further characterization of the ADAM33 enzyme.

ADAM33 contains a Zn^{2+} ion in its active site, which plays an essential role for the metalloproteinase catalytic activity, and Ca^{2+} ion for its structural stability (*19*). Thus, effects of these ions on ADAM33 activity were evaluated. With increasing concentrations of Zn^{2+}, reduced enzyme activity was observed, probably due to a competition effect (Figure 5A). With a Ca^{2+} concentration of less than 10 mM, ADAM33 activity was sharply inversely related to the Ca^{2+}

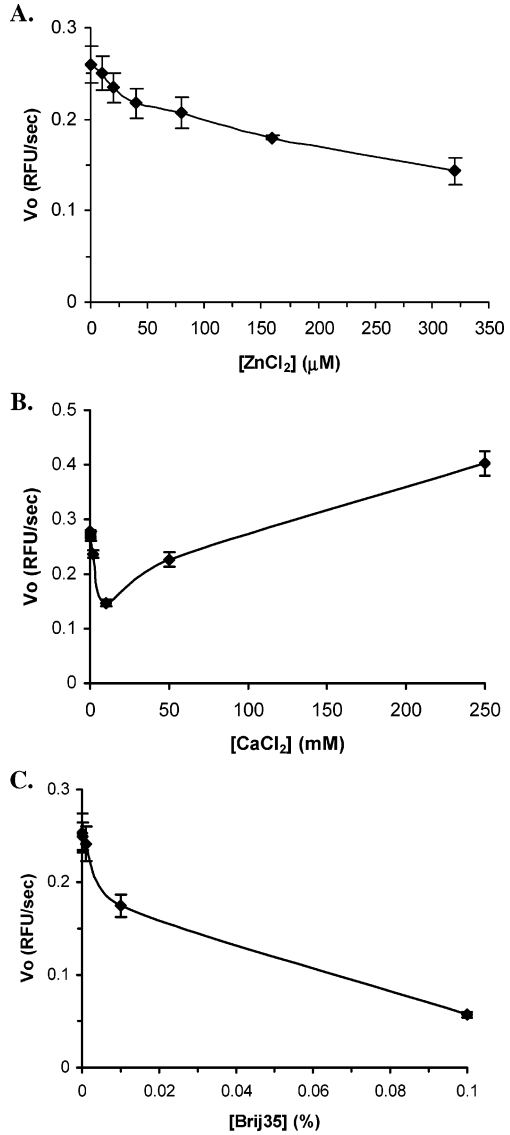

FIGURE 5: Effect of $ZnCl_2$ (A), $CaCl_2$ (B), and Brij35 (C) concentrations on ADAM33 protease activity. The fluorogenic substrate FRET-P2 [K(Dabcyl)YRVAF*QKLAE(Edans)K] was used to measure ADAM33 enzyme activity by the FRET assay. The experiments were performed using 10 nM enzyme and 30 μM substrates in the core buffer of 20 mM HEPES at pH 7.0 and RT (see Materials and Methods). The initial reaction velocity (V_o) was measured as relative fluorescence units per second (RFU/s).

concentration. However, with a Ca^{2+} concentration of >10 mM, ADAM33 activity was directly proportional to the Ca^{2+} concentration (up to 250 mM) (Figure 5B). In addition, detergents known to stabilize membrane proteins were also examined for their influence on ADAM33 catalytic domain activity. Figure 5C illustrates that ADAM33 activity decreased with increasing concentrations of nonionic detergent Brij35. The loss of activity was more pronounced at Brij35 concentrations below its critical micellar concentration (CMC) of 0.01%. A similar inverse relationship of ADAM33 activity with detergents CHAPS (zwitterionic) and lauryl β-D-maltoside (nonionic) was observed (data not shown). ADAM33 activity was increased ~30% with the addition of BSA up to 1 mg/mL (data not shown). In addition, there was no significant effect on ADAM33 activity of DMSO (0−5%) or glycerol (0−10%) (data not shown).

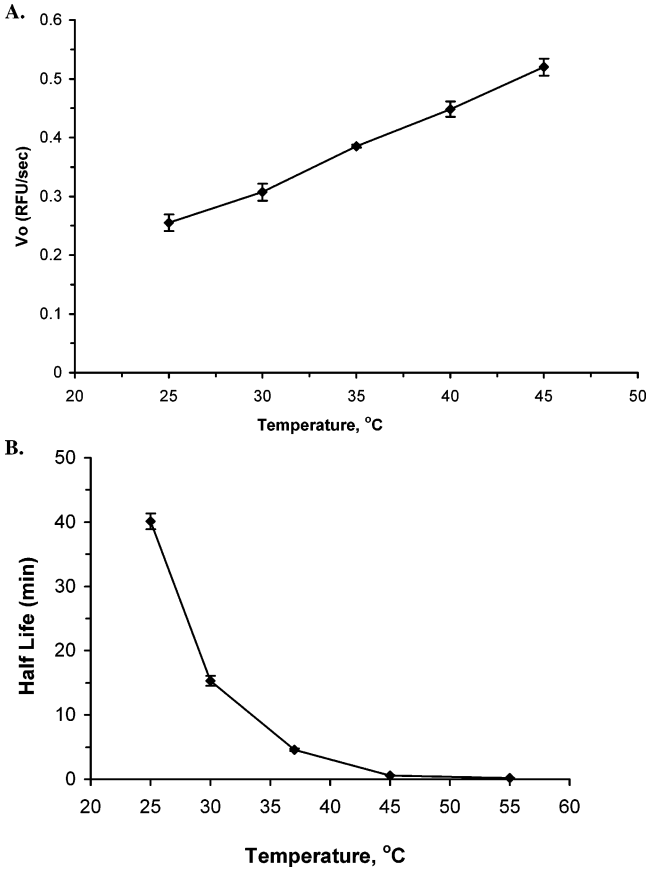

FIGURE 6: (A) Temperature dependence of ADAM33 protease activity. The initial cleavage velocity (V_o) of the substrate FRET-P2 [K(Dabcyl)YRVAF*QKLAE(Edans)K] was determined at each temperature in the assay buffer [20 mM HEPES (pH 7.0) and 0.5 M NaCl] with a GEMINI fluorescence reader. (B) Temperature dependence of the half-life of ADAM33 enzyme activity. ADAM33 (80 nM) was incubated at 25, 30, 37, 45, and 55 °C in the assay buffer. At each time point, aliquots were removed and frozen at −80 °C; samples were later diluted 10-fold to measure their protease activity. The curve summarizing the decay of protease activity with time was used to estimate the half-life of the activity at different temperature (see Materials and Methods). The half-lives of ADAM33 were 40 min at 25 °C, 15 min at 30 °C, 5 min at 37 °C, and ~1 min at 45 °C.

Temperature Dependence of ADAM33 Activity. To examine the effect of temperature on ADAM33 protease activity, the initial rate of substrate cleavage was measured between 25 and 45 °C. As shown in Figure 6A, there was a linear increase in ADAM33 enzyme activity with an increase in temperature; ADAM33 activity nearly doubled between 25 and 37 °C. The effect of prolonged preincubation at different temperatures on ADAM33 protease activity was also examined. It was noticed that ADAM33 activity decreased with preincubation at ≥25 °C, with a faster decrease at higher temperatures. The half-life of the ADAM33 enzyme was sharply reduced from 40 min at 25 °C to 5 min at 37 °C (Figure 6B).

In addition, the initial rate of substrate cleavage at 25 °C was measured at different concentrations of the enzyme. The ADAM33 activity was proportional to increasing enzyme concentrations and was linear in the range of 10−60 nM (Figure 7A). ADAM33 activity was also increased with the substrate concentration and fit to simple Michaelis−Menten kinetics. A plot of ADAM33 activity versus the substrate FRET-P2 is shown in Figure 7B. ADAM33 had the follow-

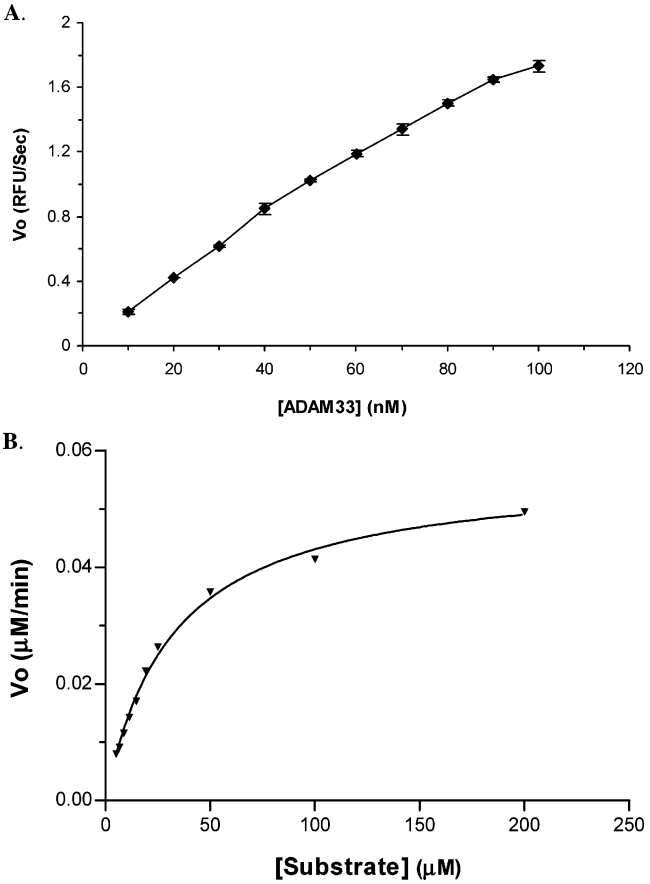

FIGURE 7: (A) Dependence of the initial velocity of ADAM33 protease activity on the concentration of ADAM33. The reaction was performed in the assay buffer [20 mM HEPES (pH 7.5) and 0.5 M NaCl] with 30 μM substrate FRET-P2 [K(Dabcyl)-YRVAF*QKLAE(Edans)K] at RT. (B) Kinetic analysis of ADAM33 protease activity by the HPLC assay. ADAM33 (4 nM) was incubated with the substrate FRET-P2 (5−200 μM) in assay buffer for 10−60 min at RT. The amount of the cleaved substrate was determined by the HPLC assay (see Materials and Methods). The kinetic constants were determined on the basis of the best fit of the data with the Michaelis−Menten equation (*26*): $k_{cat} = 1.2 \pm 0.1$ s^{-1}, $K_m = 31.8 \pm 0.4$ μM, and $k_{cat}/K_m = (3.6 \pm 0.1) \times 10^4$ s^{-1} M^{-1}.

ing apparent kinetic constants: $k_{cat} = 1.2 \pm 0.1$ s^{-1}, $K_m = 31.8 \pm 0.4$ μM, and $k_{cat}/K_m = (3.6 \pm 0.1) \times 10^4$ s^{-1} M^{-1}.

The effects of natural and synthetic MMP inhibitors on ADAM33 protease activity were tested by the optimized FRET assay. Whereas no inhibition by TIMP-1 was observed, the K_i values (mean ± SD) for TIMP-2−4 were 660 ± 150 nM ($n = 2$), 7 ± 1 nM ($n = 3$), and 40 ± 10 nM ($n = 2$), respectively. The K_i values for the hydroxamate-based compounds IK682 (*20*) and marimastat (*21*) were determined to be 15 ± 3 nM ($n = 3$) and 120 ± 30 nM ($n = 2$), respectively.

DISCUSSION

In this study, we report the establishment of a substrate specificity profile and enzymatic characterization of the human ADAM33 metalloproteinase. To probe peptide specificity, the APP peptide, YEVHH*QKLAF, was used as a model system and a template sequence for amino acid replacement studies. The C-terminal and N-terminal amino acids of the APP peptide were systematically removed or extended, which revealed that the minimal size required for ADAM33-mediated cleavage was the P5−P4′ peptide, although not all nine residues are equally important. Full positional scanning revealed that the three most stringent residues are P3 Val, P2 Ala, and P1′ Gln, and are likely to be in most direct contact with the substrate-binding pockets in ADAM33. The least stringent position is P4, accommodating almost all residues except Gly or Trp. Four other positions (P5, P1, P2′, and P4′) appear to favor mostly hydrophobic residues (aromatic or aliphatic). However, no synergistic enhancement was observed when two or more of these "good" residues at P5, P1, P2′, and P4′ were combined into a single peptide sequence in the context of the most stringent residues mentioned above (data not shown). It is postulated that different combinations of residues interact differently with their conformationally plastic protein partners. Similar context-dependent conformational effects have been observed (*30*−*32*).

The substrate specificity profile made it possible to generate a significantly improved substrate through a combination of amino acid substitutions. The best substrate, FRET-P2 [K(Dabcyl)YRVAF*QKLAE(Edans)K], was cleaved ~100-fold more efficiently than the wild-type APP peptide substrate, with a k_{cat}/K_m value of $(3.6 \pm 0.1) \times 10^4$ s^{-1} M^{-1}. This is similar to the k_{cat}/K_m values of peptide substrates of ADAM proteases: ADAM17 cleavage of proTNF-α peptide (1.7×10^5 s^{-1} M^{-1}) (*29*) or ADAM9 cleavage of proTNF-α peptide and APP (2×10^5 and 6×10^4 s^{-1} M^{-1}, respectively) (*23*). The ADAM33 cleavage efficiency of FRET-P2 was within 10-fold of the k_{cat}/K_m values of the best substrates of some ADAMs.

Using this substrate and a fluorescence resonance energy transfer (FRET) assay, ADAM33 protease activity and its sensitivity to various factors, such as pH and ionic strength, were studied. Interestingly, two substrates, FRET-P1 and FRET-P2, showed distinct profiles of pH dependence and NaCl concentration dependence (Figure 4A,B), and this was caused by the two amino acid substitutions that differed between the two substrates: Glu to Arg at P4 and His to Phe at P1. It is likely that the more important difference is His at P1 of FRET-P1 which appears to titrate at pH ~6.5−7.0. The positively charged form at lower pH was a poorer substrate; especially at the P1 residue, the enzyme is probably very sensitive to charge here. A higher salt concentration could help neutralize the unfavorable effects of this positive charge. In contrast, the P4 residue is distant from the catalytic center and solvent exposed so that the Glu to Arg change is likely less important. Further study is needed to understand the interaction between these substrates and the enzyme.

The ADAM33 active site contains a catalytic Zn^{2+} ion, which is coordinated by a water molecule and the three histidine residues in a zinc-binding motif, HEXXHXXGXXH (*19*). Within the motif, the conserved Glu346 presumably can activate zinc-coordinated water which in turn acts as a nucleophile attacking the carbonyl carbon of a peptide scissile bond of the substrate (*33*). In this study, it was found that the Zn^{2+} concentration inversely affected ADAM33 protease activity. It is possible that free Zn^{2+} ion in buffer may directly compete with ADAM33-bound catalytic Zn^{2+} ion, thus interfering with the peptide hydrolysis reaction. There are several reports that matrix metalloproteinases also require calcium for stability and activity (*34*, *35*). For instance, Housley et al. demonstrated that calcium was essential for

stability and correct processing of pro-MMP-3 into the low- or high-mass MMP-3 active species and for thermostability of the low-mass catalytic domain (*34*). Previous X-ray structure analysis of ADAM33 revealed that its catalytic domain contained a Ca^{2+} ion, which may be important for its structural stability (*19*). Our experimental data indicated that the concentration of calcium affected ADAM33 activity. We hypothesize that the purified catalytic domain of ADAM33 is stabilized by a higher concentration of calcium, which may in turn enhance the enzyme activity.

ADAM33 is an integral membrane protein. To study its protease properties, a recombinant form of the ADAM33 catalytic domain was isolated and the X-ray structure was obtained (*19*), as was done for ADAM17 (*36*) and ADAM19 (*11*). To measure protease activity of ADAMs, it is typical to include a detergent in the assay buffer to stabilize the diluted enzyme. For example, nonionic detergent Brij35 was used in activity measurements of ADAM8 (*37*), ADAM15 (*37*), ADAM28 (*37*), ADAM17 (*29*, *38*), and ADAM19 (*39*). Alternatively, the zwitterionic detergent CHAPS was used for ADAM8 (*40*) and ADAM12 (*41*). During our optimization of ADAM33 assay conditions, several detergents known to stabilize membrane protein were tested, including Brij35, lauryl β-D-maltoside, and CHAPS. However, none improved ADAM33 activity; rather, some had an adverse effect. It was likely that these detergents interfered with the enzyme's interaction with the substrate which was labeled with Edans and Dabcyl. A similar substrate, labeled with a different fluorophore and quencher, was not affected by detergents. Nevertheless, our final optimal condition of the ADAM33 assay with the substrate FRET-P2 does not include any detergents.

The thermostability of the ADAM33 catalytic domain was also studied, and temperature dependence data revealed that the catalytic activity of ADAM33 was higher at 37 °C than at 25 °C. However, the half-life of the enzyme was significantly shorter at the higher temperature. This instability is most likely due to it being an isolated catalytic domain alone in the buffer system instead of a whole protein in its native membrane physiological environment. In addition, it is likely that the half-life of the enzyme was underestimated to some degree since the procedure of freezing and thawing of the enzyme at the end of the preincubation period at each temperature may partially inactivate the enzyme. Nevertheless, the assay of ADAM33 activity is preferably set at 25 °C for reasons of both convenience and prolonged enzyme life.

Last, the sensitivity of ADAM33 protease activity to TIMP inhibitors and hydroxamate-based compounds (*16*) was reexamined with the optimized FRET assay. The K_i values that were obtained were in general agreement with those obtained by HPLC analysis with a low-efficiency peptide substrate, KL-1 [$k_{cat}/K_m = (2.6 \pm 0.5) \times 10^2$ s^{-1} M^{-1}] (*16*). Since the substrate FRET-P2 is ~100-fold more efficient than KL-1, the current FRET assay is much more sensitive than the previous HPLC assay and uses only one-twentieth to one-eightieth of the amount of enzyme used before. This is a significant advantage in reducing systematic errors and lowering the detection limit for determining the "tight-binding" inhibition constant where the enzyme concentration is approximately equal to, or even higher than, the apparent inhibition constant (*27*). Thus, the K_i values (mean ± SD) for TIMP-2−4 as determined by the FRET assay were 660 ± 150, 7 ± 1, and 40 ± 10 nM, respectively, which would be considered to be closer to their true values than the K_i values obtained previously by HPLC analysis (1400 ± 300, 60 ± 20, and 220 ± 20 nM, respectively) (*16*). As a comparison, the K_i values for TIMP-2−4 in the ADAM17 FRET assay were 11 ± 0.9, 1.1 ± 0.5, and 92 ± 25 nM, respectively (*16*). Similarly, the inhibition constants for the hydroxamate-based inhibitors determined by the FRET assay were 15 ± 3 nM for IK682 and 120 ± 30 nM for marimastat, whereas the K_i values by previous HPLC analysis were 23 ± 7 nM for IK682 and 160 ± 40 nM for marimastat (*16*).

In summary, for the first time, we have established a substrate specificity profile for the ADAM33 enzyme and generated a highly efficient peptide substrate with ~100-fold greater efficiency than the previous peptide substrate. A sensitive and rapid FRET assay was developed and used to define several important characteristics of ADAM33 protease activity, including the enzyme thermal stability, the pH optima, the ionic strength effects, and the minimum substrate size. More accurate K_i values for TIMP inhibitors and small molecule compounds were obtained.

ACKNOWLEDGMENT

We thank Dr. W. Windsor and J. Durkin for support and peptide synthesis, Drs. P. Orth and L. Xiao for the X-ray structure of ADAM33, and Drs. C. Garlisi, W. Wang, M. Billah, R. Egan, S. Taremi, and H. Le for support and many helpful discussions.

REFERENCES

1. Van Eerdewegh, P., Little, R. D., Dupuis, J., Del Mastro, R. G., Falls, K., Simon, J., Torrey, D., Pandit, S., McKenny, J., Braunschweiger, K., Walsh, A., Liu, Z., Hayward, B., Folz, C., Manning, S. P., Bawa, A., Saracino, L., Thackston, M., Benchekroun, Y., Capparell, N., Wang, M., Adair, R., Feng, Y., Dubois, J., FitzGerald, M. G., Huang, H., Gibson, R., Allen, K. M., Pedan, A., Danzig, M. R., Umland, S. P., Egan, R. W., Cuss, F. M., Rorke, S., Clough, J. B., Holloway, J. W., Holgate, S. T., and Keith, T. P. (2002) Association of the *ADAM33* gene with asthma and bronchial hyperresponsiveness, *Nature 418*, 426−430.
2. Seals, D. F., and Courtneidge, S. A. (2003) The ADAMs family of metalloproteases: Multidomain proteins with multiple functions, *Genes Dev. 17*, 7−30.
3. Black, R. A., and White, J. M. (1998) ADAMs: Focus on the protease domain, *Curr. Opin. Cell Biol. 10*, 654−659.
4. Becherer, J. D., and Blobel, C. P. (2003) Biochemical properties and functions of membrane-anchored metalloprotease-disintegrin proteins (ADAMs), *Curr. Top. Dev. Biol. 54*, 101−123.
5. Blobel, C. P. (2000) Remarkable roles of proteolysis on and beyond the cell surface, *Curr. Opin. Cell Biol. 12*, 606−612.
6. Black, R. A., Rauch, C. T., Kozlosky, C. J., Peschon, J. J., Slack, J. L., Wolfson, M. F., Castner, B. J., Stocking, K. L., Reddy, P., Srinivasan, S., Nelson, N., Boiani, N., Schooley, K. A., Gerhart, M., Davis, R., Fitzner, J. N., Johnson, R. S., Paxton, R. J., March, C. J., and Cerretti, D. P. (1997) A metalloproteinase disintegrin that releases tumour-necrosis factor-α from cells, *Nature 385*, 729−733.
7. Buxbaum, J. D., Liu, K. N., Luo, Y., Slack, J. L., Stocking, K. L., Peschon, J. J., Johnson, R. S., Castner, B. J., Cerretti, D. P., and Black, R. A. (1998) Evidence that tumor necrosis factor α converting enzyme is involved in regulated α-secretase cleavage of the Alzheimer amyloid protein precursor, *J. Biol. Chem. 273*, 27765−27767.
8. Peschon, J. J., Slack, J. L., Reddy, P., Stocking, K. L., Sunnarborg, S. W., Lee, D. C., Russell, W. E., Castner, B. J., Johnson, R. S., Fitzner, J. N., Boyce, R. W., Nelson, N., Kozlosky, C. J., Wolfson, M. F., Rauch, C. T., Cerretti, D. P., Paxton, R. J., March, C. J.,

and Black, R. A. (1998) An essential role for ectodomain shedding in mammalian development, *Science 282*, 1281−1284.
9. Yoshinaka, T., Nishii, K., Yamada, K., Sawada, H., Nishiwaki, E., Smith, K., Yoshino, K., Ishiguro, H., and Higashiyama, S. (2002) Identification and characterization of novel mouse and human ADAM33s with potential metalloprotease activity, *Gene 282*, 227−236.
10. Gunn, T. M., Azarani, A., Kim, P. H., Hyman, R. W., Davis, R. W., and Barsh, G. S. (2002) Identification and preliminary characterization of mouse *Adam33*, *BMC Genet. 3*, 2.
11. Chesneau, V., Becherer, J. D., Zheng, Y., Erdjument-Bromage, H., Tempst, P., and Blobel, C. P. (2003) Catalytic Properties of ADAM19, *J. Biol. Chem. 278*, 22331−22340.
12. Shirakabe, K., Wakatsuki, S., Kurisaki, T., and Fujisawa-Sehara, A. (2001) Roles of Meltrin β/ADAM19 in the processing of neuregulin, *J. Biol. Chem. 276*, 9352−9358.
13. Asakura, M., Kitakaze, M., Takashima, S., Liao, Y., Ishikura, F., Yoshinaka, T., Ohmoto, H., Node, K., Yoshino, K., Ishiguro, H., Asanuma, H., Sanada, S., Matsumura, Y., Takeda, H., Beppu, S., Tada, M., Hori, M., and Higashiyama, S. (2002) Cardiac hypertrophy is inhibited by antagonism of ADAM12 processing of HB-EGF: Metalloproteinase inhibitors as a new therapy, *Nat. Med. 8*, 35−40.
14. Loechel, F., Fox, J. W., Murphy, G., Albrechtsen, R., and Wewer, U. M. (2000) ADAM 12-S cleaves IGFBP-3 and IGFBP-5 and is inhibited by TIMP-3, *Biochem. Biophys. Res. Commun. 278*, 511−515.
15. Garlisi, C. G., Zou, J., Devito, K. E., Tian, F., Zhu, F. X., Liu, J., Shah, H., Wan, Y., Billah, M. M., Egan, R. W., and Umland, S. P. (2003) Human ADAM33: Protein maturation and localization, *Biochem. Biophys. Res. Commun. 301*, 35−43.
16. Zou, J., Zhu, F., Liu, J., Wang, W., Zhang, R., Garlisi, C. G., Liu, Y. H., Wang, S., Shah, H., Wan, Y., and Umland, S. P. (2004) Catalytic activity of human ADAM33, *J. Biol. Chem. 279*, 9818−9830.
17. Umland, S. P., Garlisi, C. G., Shah, H., Wan, Y., Zou, J., Devito, K. E., Huang, W. M., Gustafson, E. L., and Ralston, R. (2003) Human ADAM33 Messenger RNA Expression Profile and Post-transcriptional Regulation, *Am. J. Respir. Cell Mol. Biol. 29*, 571−582.
18. Davies, D. E., Wicks, J., Powell, R. M., Puddicombe, S. M., and Holgate, S. T. (2003) Airway remodeling in asthma: New insights, *J. Allergy Clin. Immunol. 111*, 215−225.
19. Orth, P., Reichert, P., Wang, W., Prosise, W. W., Yarosh-Tomaine, T., Hammond, G., Ingram, R. N., Xiao, L., Mirza, U. A., Zou, J., Strickland, C., Taremi, S. S., Le, H. V., and Madison, V. (2004) Crystal structure of the catalytic domain of human ADAM33, *J. Mol. Biol. 335*, 129−137.
20. Duan, J. J., Chen, L., Wasserman, Z. R., Lu, Z., Liu, R. Q., Covington, M. B., Qian, M., Hardman, K. D., Magolda, R. L., Newton, R. C., Christ, D. D., Wexler, R. R., and Decicco, C. P. (2002) Discovery of γ-lactam hydroxamic acids as selective inhibitors of tumor necrosis factor α converting enzyme: Design, synthesis, and structure−activity relationships, *J. Med. Chem. 45*, 4954−4957.
21. Rasmussen, H. S., and McCann, P. P. (1997) Matrix metalloproteinase inhibition as a novel anticancer strategy: A review with special focus on batimastat and marimastat, *Pharmacol. Ther. 75*, 69−75.
22. Erdjument-Bromage, H., Lui, M., Sabatini, D. M., Snyder, S. H., and Tempst, P. (1994) High-sensitivity sequencing of large proteins: Partial structure of the rapamycin-FKBP12 target, *Protein Sci. 3*, 2435−2446.
23. Roghani, M., Becherer, J. D., Moss, M. L., Atherton, R. E., Erdjument-Bromage, H., Arribas, J., Blackburn, R. K., Weskamp, G., Tempst, P., and Blobel, C. P. (1999) Metalloprotease-disintegrin MDC9: Intracellular maturation and catalytic activity, *J. Biol. Chem. 274*, 3531−3540.
24. Park, H. I., Turk, B. E., Gerkema, F. E., Cantley, L. C., and Sang, Q. X. (2002) Peptide substrate specificities and protein cleavage sites of human endometase/matrilysin-2/matrix metalloproteinase-26, *J. Biol. Chem. 277*, 35168−35175.
25. Zhang, R., Beyer, B. M., Durkin, J., Ingram, R., Njoroge, F. G., Windsor, W. T., and Malcolm, B. A. (1999) A continuous spectrophotometric assay for the hepatitis C virus serine protease, *Anal. Biochem. 270*, 268−275.
26. Lehninger, A. L. (1975) *Biochemistry*, 2nd ed., Worth Publishers, Inc., New York.
27. Kuzmic, P., Elrod, K. C., Cregar, L. M., Sideris, S., Rai, R., and Janc, J. W. (2000) High-throughput screening of enzyme inhibitors: Simultaneous determination of tight-binding inhibition constants and enzyme concentration, *Anal. Biochem. 286*, 45−50.
28. Williams, J. W., and Morrison, J. F. (1979) The kinetics of reversible tight-binding inhibition, *Methods Enzymol. 63*, 437−467.
29. Mohan, M. J., Seaton, T., Mitchell, J., Howe, A., Blackburn, K., Burkhart, W., Moyer, M., Patel, I., Waitt, G. M., Becherer, J. D., Moss, M. L., and Milla, M. E. (2002) The tumor necrosis factor-α converting enzyme (TACE): A unique metalloproteinase with highly defined substrate selectivity, *Biochemistry 41*, 9462−9469.
30. Padmanabhan, S., Marqusee, S., Ridgeway, T., Laue, T. M., and Baldwin, R. L. (1990) Relative helix-forming tendencies of nonpolar amino acids, *Nature 344*, 268−270.
31. Chakrabartty, A., Schellman, J. A., and Baldwin, R. L. (1991) Large differences in the helix propensities of alanine and glycine, *Nature 351*, 586−588.
32. Serrano, L., Neira, J. L., Sancho, J., and Fersht, A. R. (1992) Effect of alanine versus glycine in α-helices on protein stability, *Nature 356*, 453−455.
33. Coleman, J. E. (1998) Zinc enzymes, *Curr. Opin. Chem. Biol. 2*, 222−234.
34. Housley, T. J., Baumann, A. P., Braun, I. D., Davis, G., Seperack, P. K., and Wilhelm, S. M. (1993) Recombinant Chinese hamster ovary cell matrix metalloprotease-3 (MMP-3, stromelysin-1). Role of calcium in promatrix metalloprotease-3 (pro-MMP-3, prostromelysin-1) activation and thermostability of the low mass catalytic domain of MMP-3, *J. Biol. Chem. 268*, 4481−4487.
35. Okada, Y., Nagase, H., and Harris, E. D., Jr. (1986) A metalloproteinase from human rheumatoid synovial fibroblasts that digests connective tissue matrix components. Purification and characterization, *J. Biol. Chem. 261*, 14245−14255.
36. Milla, M. E., Leesnitzer, M. A., Moss, M. L., Clay, W. C., Carter, H. L., Miller, A. B., Su, J. L., Lambert, M. H., Willard, D. H., Sheeley, D. M., Kost, T. A., Burkhart, W., Moyer, M., Blackburn, R. K., Pahel, G. L., Mitchell, J. L., Hoffman, C. R., and Becherer, J. D. (1999) Specific sequence elements are required for the expression of functional tumor necrosis factor-α-converting enzyme (TACE), *J. Biol. Chem. 274*, 30563−30570.
37. Fourie, A. M., Coles, F., Moreno, V., and Karlsson, L. (2003) Catalytic activity of ADAM8, ADAM15 and MDC-L (ADAM28) on synthetic peptide substrates, and in ectodomain cleavage of CD23, *J. Biol. Chem. 278*, 30469−30477.
38. Jin, G., Huang, X., Black, R., Wolfson, M., Rauch, C., McGregor, H., Ellestad, G., and Cowling, R. (2002) A continuous fluorimetric assay for tumor necrosis factor-α converting enzyme, *Anal. Biochem. 302*, 269−275.
39. Kang, T., Park, H. I., Suh, Y., Zhao, Y. G., Tschesche, H., and Sang, Q. X. (2002) Autolytic processing at Glu586-Ser587 within the cysteine-rich domain of human adamalysin 19/disintegrin-metalloproteinase 19 is necessary for its proteolytic activity, *J. Biol. Chem. 277*, 48514−48522.
40. Schlomann, U., Wildeboer, D., Webster, A., Antropova, O., Zeuschner, D., Knight, C. G., Docherty, A. J., Lambert, M., Skelton, L., Jockusch, H., and Bartsch, J. W. (2002) The metalloprotease disintegrin ADAM8. Processing by autocatalysis is required for proteolytic activity and cell adhesion, *J. Biol. Chem. 277*, 48210−48219.
41. Loechel, F., and Wewer, U. M. (2001) Activation of ADAM 12 protease by copper, *FEBS Lett. 506*, 65−68.

BI0476230